ISSN 0967-0912, Steel in Translation, 2016, Vol. 46, No. 11, pp. 792–797. © Allerton Press, Inc., 2016.
Original Russian Text © A.M. Avdeenko, V.G. Molyarov, A.V. Kalashnikova, A.N. Bocharov, A.V. Molyarov, 2016, published in Izvestiya Vysshikh Uchebnykh Zavedenii, Chernaya Metallurgiya, 2016, No. 11, pp. 826–832.

Strong Bimetallic Structural Material Alloyed with Nitrogen

A. M. Avdeenko[a], *, V. G. Molyarov[b], **, A. V. Kalashnikova[b], *, A. N. Bocharov[b], ****, and A. V. Molyarov[c], *******

[a]*Academy of the State Fire-Prevention Service, Russian Ministry of Emergency Situations, Moscow, Russia*
[b]*AO VNIINEFTEMASh, Moscow, Russia*
[c]*Moscow Institute of Steel and Alloys, Moscow, Russia*
**e-mail: desperados67@inbox.ru*
***e-mail: molyaron@mail.ru*
****e-mail: 4657952@mail.ru*
*****e-mail: bocharov.albert@yandex.ru*
******e-mail: anwil_875@mail.ru*

Received June 23, 2016

Abstract—The production of strong two-layer steel sheet—a bimetallic structure with a basic layer of low-carbon manganese microalloyed bainitic steel and an applied layer of two-phase austenite–ferrite stainless steel alloyed with nitrogen—is considered. In trials, the production of bimetallic material on the basis of the electrical-arc surfacing is investigated: specifically, the application of high-alloy steel to a plane microalloyed steel blank, by means of welding wire (under a flux layer), with subsequent hot deformation. The trials include the simulation of forced sheet cooling on the exit conveyer of the broad-strip mill and slow cooling of the final coiled strip. The microstructure, mechanical strength, and corrosion resistance of the bimetallic structural material are investigated. The proposed material matches the corrosion resistance of existing bimetals. Its yield point and the adhesive strength of the two layers exceed those of traditional two-layer steel by at least 30–50% and are three times the standard requirements.

Keywords: bimetallic structural material, austenite–ferrite duplex steel, high-strength microalloyed steel, surfacing under flux, hot rolling, microstructure, mechanical properties, pitting, corrosion resistance

DOI: 10.3103/S0967091216110024

There is growing interest in nitrogen-alloyed stainless steel, which is stronger than traditional steel and also has an improved cold-brittleness threshold. That permits decrease in the mass of strong structures and reduction in the metal consumption. Nitrogen greatly stabilizes austenite and compensates for the deficiencies of nickel and manganese, which are expensive alloying elements. Their content in the steel is reduced by almost half when nitrogen is introduced [1–3].

The cost of the steel may be reduced by a further 10–25%, with 25–50% increase in strength if we switch to bimetallic composites with an applied corrosion-resistant layer and a strong structural layer that absorbs the working loads and guarantees reliable operation. The basic layer may be made of low-alloy bainitic steel, such as low-carbon microalloyed S700MC steel produced by PAO Severstal' [4–7]. Despite the constraints on the operating temperatures (no higher than 300–350°C), austenite–ferrite duplex steel alloyed with nitrogen and molybdenum is promising for the applied layer in the composite: it is strong and resistant to corrosion by alkaline media and chlorides [8]. Such steel is effective in the manufacture of equipment for the petrochemical industry (columns, heat exchangers).

Bimetallic stainless steel may be produced by forging, rolling, explosive welding, and multilayer surfacing under slag [9, 10]. In assessing these methods, we must take account not only of the quality of the material but also of economic considerations, the potential for mass production, and the environmental impact. The quality and properties of bimetallic steels depend on the binding strength of two layers, which must exceed 300 MPa. Electroslag and electric-arc surfacing best meet the latter requirement [11]. High strength improves the performance of the composite steel and hinders its disintegration. In addition, the performance of the composite steel is not greatly affected by the quality of the surface to which the second layer is applied. No defects (cracks, peeling, gaps) are observed at the boundary. With optimal selection of the surfacing conditions and the slag, a low content of nonmetallic inclusions, sulfur, and phosphorus may be ensured. That improves the mechanical and corrosional properties of the material [1, 3, 11].

Table 1. Chemical composition of the basic and applied layers in the bimetallic steel

Layer	Content, %														
	C	Si	Mn	P	S	Cr	Ni	Mo	Cu	Al	Ti	V	Nb	B	N
Base	0.08	0.15	1.95	0.008	0.003	0.04	0.12	0.23	0.09	0.04	0.08	0.04	0.06	0.003	0.05
Duplex steel	0.03	0.66	1.39	0.015	0.003	21.50	8.00	2.95	0.11	0.05	0.05	0.04	0.04	0.002	0.13

In the present work, we create a bimetallic composite on the basis of low-carbon manganese microalloyed steel, with the application of nitrogen-alloyed austenite–ferrite duplex stainless steel. We develop a production technology for this bimetallic steel by application of the high-alloy layer and subsequent deformation and heat treatment.

As the base of the bimetallic steel, we use two 200 × 50 × 12 mm plates cut from hot-rolled S700MC steel with fine-grain structure and a yield point of ~700 MPa, thanks to the bainite component formed in polymorphic γ–α transformation of the steel in accelerated cooling on the output conveyer of the 2000 broad-strip mill and also as a result of microalloying. The applied corrosion-resistant layer of austenite–ferrite duplex steel (thickness 3 and 5 mm) is applied in one and two passes, respectively, of OK Autrod 2009 welding wire (diameter 3.2 mm) under a layer of OK 10.93 flux, by automatic electric-arc welding using reversed-polarity direct current. Table 1 presents the chemical composition of each layer of the composite steel.

After 1-h holding at 1200°C, the composite steel billet (length 300 mm) is rolled to a thickness of 7 m in three passes on a DUO-300 mill, at a rate of 0.4–0.5 s^{-1}. The total reduction is ~50%; the interval between passes is no more than 5 s; and the final rolling temperatures are 780 and 840°C. Then the samples are cooled to 600°C in a water–air flux and slowly cooled in the furnace to simulate coiling of the hot-rolled strip and its subsequent thermostatting. Forced cooling of the strip from 760 and 840°C to 600°C in the final stage of hot rolling ensures quenching of the microalloyed base to bainite and stabilization of the high-temperature state of the austenite–ferrite duplex steel.

The nonmetallic inclusions and microstructure of the steel are analyzed on a Carl Zeiss Axio Lab A1 optical microscope (magnification 100–1000) and on a JEOL JSM-6610LV scanning electron microscope (magnification 1000–5000). Standard software is used for the analysis of images of the surface of unetched sections and for quantitative analysis of the nonmetallic inclusions, with noise removal and binarization. The microstructure of the steel in the basic layer of the composite is revealed by means of 3% alcoholic nitric-acid solution. The structure of the applied duplex steel is studied by electrolytic etching of sections in Waddell agent. Nanodeposits of vanadium, niobium, and titanium carbonitrides are analyzed by means of a JEOL JEM-200CX transmission electron microscope. The content of residual austenite in the basic layer is determined by X-ray diffraction on a Rigaku-X system, on the basis of the integral intensity ratio of the austenite (111) and ferrite (110) diffraction lines, to within 0.1%. The mechanical properties of the basic layer and the composite steel are determined by uniaxial static extension of standard samples at room temperature using a ZD/10/90 rupture machine.

In the initial state, the S700MC steel is characterized by fine-grain lower-bainite structure (Fig. 1). As a result of hot rolling and subsequent forced cooling of the composite steel strip to 600°C (simulation of strip coiling), upper bainite structure is formed. On quenching to bainite, low-carbon microalloyed S700MC steel has good mechanical properties. The shear strength is controlled by the diffusion of carbon, in contrast to martensitic transformation. The type of bainite structure is determined by the method of plastic accommodation: twinning produces lower bainite, while plastic slip produces upper bainite.

The upper bainite in the basic layer of the bimetallic steel has an arch structure and may be regarded as ferrite needles [12]. In the absence of packets, the fracture facets produced will pass through the whole of the former austenite grain. The nucleation of facets is facilitated by the presence of carbides at the grain boundaries. Therefore, in order to increase the yield point and the impact strength of this steel, it is expedient to keep the austenite grain size below a score of 9, by controlled rolling.

The length of the disoriented ferrite needles varies from section to section. The proportion of the residual austenite is no more than 1%. We see many chains of V(CN), Nb(CN), and Ti(CN) nanodeposits of dimensions 10–100 nm in the ferrite, which ensures dispersional hardening of the basic layer. The content of corrosive nonmetallic inclusions in S700MC steel is within the limit of two particles per mm^2 that was established for low-carbon steel with high resistance to local corrosion.

The applied austenite–ferrite duplex steel has dendritic structure in the form of columnar crystals oriented along the temperature gradient of the solidifying melt (Fig. 2a). After thermodeformational treatment of the composite steel with ~50% reduction, the den-

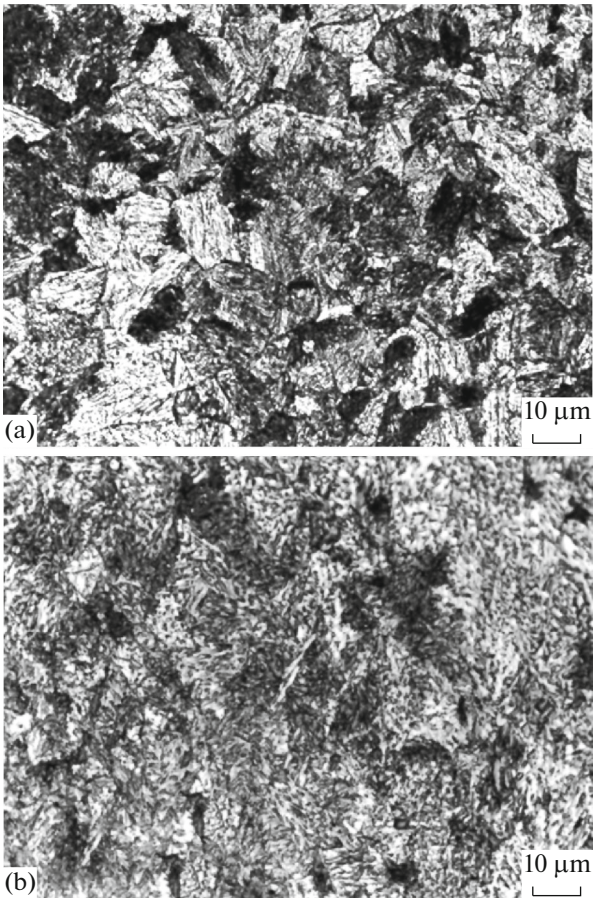

Fig. 1. Microstructure of S700MC steel (×500): (a) initial; state; (b) after hot rolling and cooling of the composite steel.

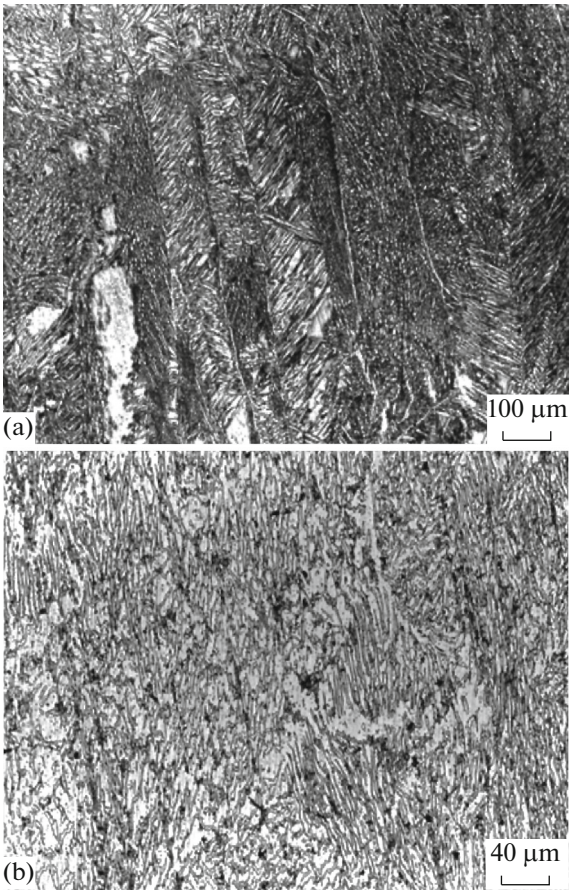

Fig. 2. Microstructure of austenite–ferrite duplex steel: (a) in cast state (×100); (b) after hot rolling with 50% reduction (×200).

dritic structure is converted to laminar structure, in which the extended grains (fibers) are mainly oriented in the direction of rolling (Fig. 2b). The main phases present are austenite and ferrite, in a ratio of 7/3. Individual silicate inclusions and point oxides (0.3–1.0 μm) are present in the applied layer (volume content no more than 2×10^{-3}), as well as nitrides and carbonitrides (Fig. 3).

The transition zone between the steels, characterized by mixing of the layers, has a width of 50–100 μm (Fig. 4). At the basic layer, we see a decarburization zone (width 5–10 μm) due to the diffusion of carbon into the applied layer.

Mechanical tests indicate that the strength and plasticity of the hot-rolled bimetallic steel are practically the same as for sheets of the individual S700MC steel and 2209 austenite–ferrite duplex steel (Table 2). The bimetallic composite is almost 1.5 times stronger than 09G2S steel, while the plastic properties are similar. The microhardness is also similar for the basic layer and austenite–ferrite duplex steel in the composite: 2740 and 2680 N/mm^2, respectively, after one surfacing pass and 2420 and 2850 N/mm^2, respectively, after two passes. These results confirm that the two layers of the composite steel are of comparable strength.

The ductile fractures obtained in uniaxial tests of plane bimetallic-steel samples are characterized by complex relief; some exhibit peeling in the central

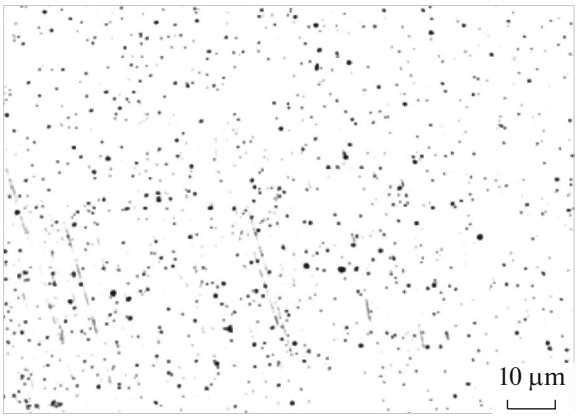

Fig. 3. Nonmetallic inclusions in the applied layer (×500).

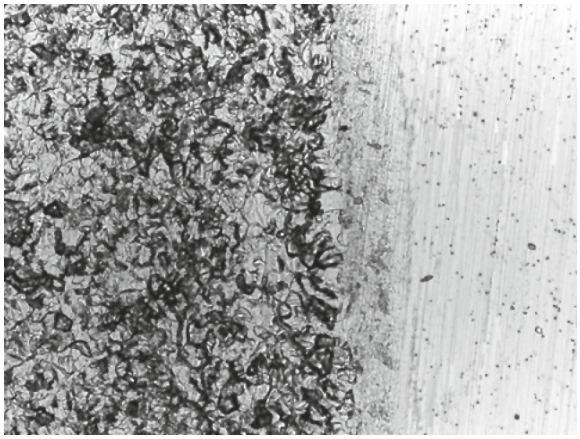

Fig. 4. Poorly distinguishable transition zone between the etched basic layer and the unetched applied layer (×500).

region (Fig. 5). This is associated with the presence of the basic, transition, and applied layers and also interlayers (the decarburization zone and the carbide layers), which have different structural states and deformation diagrams.

The adhesive strength of the two main layers in the hot-rolled composite steel is 469–478 N/mm^2 according to tests of samples with a cut applied layer. This is triple the requirement of 147 N/mm^2 in State Standard GOST 10885. That ensures high quality of the composite.

Taking account of the content of Cr, Mn, and N, we may evaluate the resistance to pitting corrosion of the austenite–ferrite duplex steel on the basis of the formula [13, 14]

$$\mathrm{PREN_N} = [\mathrm{Cr}] + 3.3[\mathrm{Mo}] + 16[\mathrm{N}].$$

We obtain a value greater than 33%, which exceeds those of 10Kh17N13M2T and 08Kh18N10T steel by factors of almost 1.5 and 2, respectively. This indicates that the applied layer has excellent resistance to pitting corrosion.

The sensitivity to pitting is predictable. The active medium always interacts with nonmetallic inclusions of specific form. For example, in low-carbon steel, pitting appears at sulfides, according to the reaction

$$\mathrm{MnS} + \mathrm{H_2SO_4} = \mathrm{MnSO_4} + \mathrm{H_2S}.$$

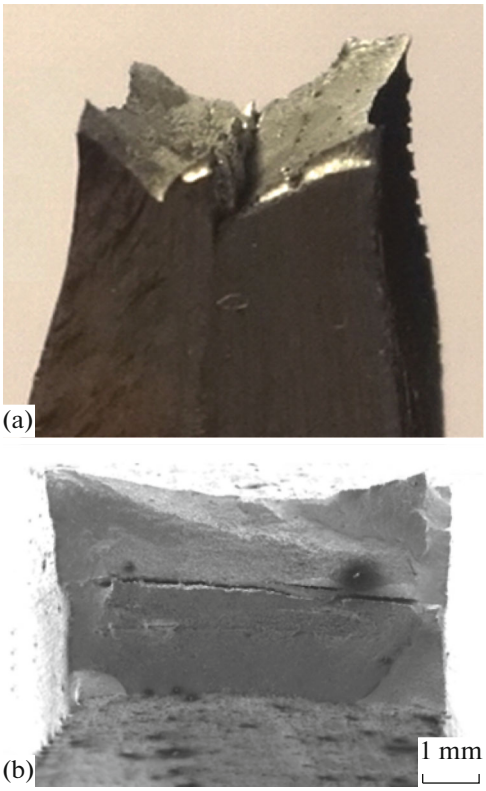

Fig. 5. Structure of fractures in bimetallic steel: (a) necking under uniaxial extension (×10); (b) peeling in the transition zone (×25).

Therefore, to prevent pitting, we need to limit the sulfur content to 0.01%, while the Mn/S ratio must be more than 50 [15]. If the inclusions are of size d and are present in the steel in a concentration n, the distance between them is

$$L_2 \sim d/n^{1/2} \text{ and } L_3 \sim d/n^{1/3},$$

at the surface of the material and in its volume, respectively. Consequently, we find that $L_2/L_3 = n^{-1/6} \approx 3$–$7$ if $n \sim 10^{-3}$–10^{-5}.

This means that $L_3 \ll L_2$. In other words, inclusions are more readily encountered in the depth of the material, and corrosion will extend into the depth. When pitting covers a proportion of the surface $(L_3/L_2)^2 \sim n^{1/3}$, the corrosion extends from inclusion to inclusion and

Table 2. Mechanical properties of hot-rolled steels

Steel	$\sigma_{0.2}$, MPa	σ_u, MPa	δ_5, %
Composite steel (S7000MC + Duplex steel)	544	658	21
S700MC	508	649	20
2205 austenite–ferrite duplex steel (foreign standard requirements)	max 460	max 700	min 25
09G2S	341	512	26

eats through the wall of the vessel. In other words, even small nonmetallic inclusions (~1 μm) may lead to active pitting, depending on their concentration. Therefore, in improving the production of composite steel, we need to reduce the content of nonmetallic inclusions in the surface layer.

Prolonged (115-h) corrosion tests of composite steel samples in 6% aqueous iron-chloride solution ($FeCl_3 \cdot 6H_2O$), with gravimetric monitoring of the mass loss of the austenite–ferrite duplex steel layer (applied in two passes), indicate that its resistance to the action of chloride ions is satisfactory. Against the background of slight mass loss of the composite steel, corrosional failure of the austenite–ferrite duplex steel layer is not observed. The mean corrosion rate of the experimental samples is 1.7 g/m^2 h.

In view of the high strength of the proposed composite steel (including the adhesive strength of its components) and its satisfactory plasticity and corrosion resistance, it is a promising alternative to a traditional 09G2S + 08KhN10T steel bimetal. Its main benefit is that the two layers are of equal strength. The compatibility of the two steels employed is better than for a traditional bimetal; the mutual adhesion of the steels in a complex stress state is greater; and strength calculations are simpler. Note that, thanks to optimal heat treatment and deformation, the upper bainite structure in the S700MC steel ensures impact strength of 0.7–0.8 MJ/m^2 at –20°C. This is 10–15% greater than in 09G2S steel and permits operation in complex conditions.

The effectiveness of the proposed bimetallic composite is confirmed by strength calculations of a cylindrical tank (length L, internal diameter a, external diameter b) under pressure P. When $L \gg b$, the cross section of the tank may be regarded as plane. Hence, the stress and strain along the z axis of the cylindrical coordinate system $\{r, z, \theta\}$ are constant

$$\sigma_{zz} = \text{const and } \varepsilon_{zz} = \text{const}.$$

The equilibrium equations for the stress take the form

$$\frac{\partial \sigma_{rr}}{\partial r} + \frac{\sigma_{zz} - \sigma_{\theta\theta}}{r} = 0;$$

$$\frac{\partial \sigma_{rz}}{\partial r} + \frac{\sigma_{zr}}{r} = 0.$$

If we integrate the latter, we obtain $\sigma_{rz} = \alpha/r$, where α depends on the type of steel.

It follows from the boundary conditions that

$$\sigma_{rz}(a) = \sigma_{rz}(b) = 0.$$

Therefore, $\sigma_{rz}(c) = 0$, when $a \le c \le b$.

If we set $\varepsilon_{rr} = dA/dr$ and $\varepsilon_{\theta\theta} = A/r$, where A is a function of r, the compatibility condition for the strain

$$\frac{d\varepsilon_{\theta\theta}}{dr} + \frac{\varepsilon_{\theta\theta} - \varepsilon_{rr}}{r} = 0$$

is automatically satisfied.

Taking account of the Young's modulus E and Poisson's ratio γ, we may write Hooke's law in the form

$$\varepsilon_{rr} = \frac{1}{E}[\sigma_{rr} - \gamma(\sigma_{rr} + \sigma_{\theta\theta})];$$

$$\varepsilon_{\theta\theta} = \frac{1}{E}[\sigma_{\theta\theta} - \gamma(\sigma_{rr} + \sigma_{\theta\theta})];$$

$$\varepsilon_{zz} = \frac{1}{E}[\sigma_{zz} - \gamma(\sigma_{rr} + \sigma_{\theta\theta})] = \text{const}.$$

If $\sigma_{rr} = Q/r$ and $\sigma_{\theta\theta} = dQ/dr$, it follows from the compatibility conditions that

$$\ddot{Q} + \frac{\dot{Q}}{r} - \frac{Q}{r^2} = 0.$$

Hence $Q = Ar + B/r$.

Taking account of the boundary conditions, we write

$$\sigma_{rr} = P\frac{a^2}{b^2 - a^2}\left(1 - \frac{b^2}{r^2}\right);$$

$$\sigma_{\theta\theta} = P\frac{a^2}{b^2 - a^2}\left(1 + \frac{b^2}{r^2}\right).$$

When $r = a$, the maximum values are

$$\sigma_{rr} = P;\ \sigma_{\theta\theta} = P\frac{a^2 + b^2}{b^2 - a^2}.$$

From Hooke's law

$$\varepsilon_{zz} = (1 - 2\gamma)P\pi\frac{a^2}{b^2 - a^2} \text{ and } \sigma_{zz} = P\frac{a^2}{b^2 - a^2}.$$

Of course, σ_{zz} does not depend on r.

To estimate the permissible structural parameters, we need to use the Mises criterion for the maximum tangential stress

$$\tau_{\max} = \sigma_{\theta\theta} - \sigma_{zz}.$$

Since $\tau_{\max} < \sigma_{0.2}/k$, where k is the margin of strength and $\sigma_{0.2}$ is the yield point of the material, we may write

$$\sigma_{0.2} > kP\frac{b^2}{b^2 - a^2} \approx kP\frac{b}{2h},$$

since the wall thickness ($h = b - a$) is usually much less than the diameter of the cylinder.

The linear mass of a structure whose density is ρ takes the form

$$m = \pi\rho\left(b^2 - a^2\right),$$

and hence

$$m > \pi k P \rho \frac{b^2}{\sigma_{0.2}}.$$

If the yield point is increased from $\sigma_{0.2}$ to $\sigma_{0.2}$, we may reduce the mass of the tank from m (09G2S steel) to m_1 (S700MC steel) on account of the decrease in wall thickness:

$$m_1 \frac{m\sigma_{0.2}}{\sigma'_{0.2}}.$$

Since the yield point is about 500 MPa for S700MC steel and 340 MPa for 09G2S steel (Table 2), the use of the stronger material reduces the mass of the structure by 47%. For a tank (length 10 m, diameter 2.5 m, wall thickness 10 mm) under a pressure of 2.5 MPa, the mass is reduced by 2.5 t. That is accompanied by some complication of the process. Another benefit of the proposed composite steel is the high strength of the basic layer, which prevents catastrophic failure in the event of corrosion cracking of the applied layer. In fact, for a cylinder under a pressure $P = 2.5–5.0$ MPa, with specified parameters and maximum stress, the critical crack size

$$h_c \approx \frac{K_{1C}}{\tau^2_{\max}} \sim \mathrm{KCU} \sim \frac{\mathrm{KCU}}{P^2}$$

is greater than the thickness of the applied layer. The basic layer retards the crack, which is a great safety benefit.

CONCLUSIONS

We have proposed a new bimetallic structural material with a basic layer of S700MC low-carbon manganese microalloyed bainitic steel and an applied layer of austenite–ferrite duplex stainless steel alloyed with nitrogen.

The adhesive strength of the two steels in the bimetallic composite is higher than in traditional bimetallic materials on account of their technological, chemical, and structural compatibility.

In trials, we have investigated the production technology, which includes surfacing under flux on a plane microalloyed steel blank and subsequent hot rolling. Final high tempering is required to ensure an optimal combination of the mechanical and corrosional properties of the material, with equal strength of the two steel layers.

ACKNOWLEDGMENTS

Financial support was provided by the Russian Ministry of Education and Science (project identifier RFMEFI57914X0079).

REFERENCES

1. *Proc. 9th Int. Conf. on High Nitrogen Steels "HNS 2006,"* Dong, H., Su, J., and Speidel, V.O., Eds., Beijing: Metall. Ind. Press, 2006.
2. Speidel, H.J.C. and Speidel, M.O., Nickel and chromium based high nitrogen alloys, *Proc. Int. Conf. on High Nitrogen Steels "HNS 2003,"* Zurich: Swiss Fed. Inst. Technol., 2003, pp. 101–112.
3. Kamachi Mudali, U., Ningshen, S., Tyagi, A.K., and Dayal, R.K., Influence of metallurgical and chemical variables on the pitting corrosion behavior of nitrogen-bearing austenitic stainless steels, *Proc. 5th Int. Conf. on High Nitrogen Steels "HNS 1998," Abstracts of Papers*, Stockholm, 1998, p. 44.
4. Kimura, M., Effect of chrome on resistance of steel pipelines to corrosion under the action of gaseous CO_2, *Curr. Adv. Mater. Proc.*, 1991, vol. 4, p. 1984.
5. Fierro, G., Ingo, G.M., and Mancia, F., XPS investigation on AISI 420 stainless steel corrosion in oil and gas well environments, *J. Mater. Sci.*, 1990, vol. 25, no. 2, pp. 1407–1415.
6. Zaitsev, A.I., Rodionova, I.G., Pavlov, A.A., Baklanova, O.N., and Lyasotskii, I.V., Development of a new generation of high-strength low-carbon microalloyed steels for the main layer of clad rolled product, *Metallurgist*, 2015, vol. 58, no. 9, pp. 909–915.
7. Harrison J.D. et al., Work of materials in acidic environments of oil wells-problems and solutions: conference report, *Br. Corros. J.*, 1992, vol. 27, p. 95.
8. Avdeenko, A., Molyarov, V., and Kalashnikova, A., Technology for preparing increased strength bimetal with a nitrogen two-phase steel cladding layer, *Metallurgist*, 2016, vol. 59, pp. 1201–1203.
9. Craig, B.D., Field experience with alloy-clad API grade L-80 tubing, *Mater. Perform.*, 1986, vol. 25, no. 6, pp. 48–50.
10. Takashi, F., Alloyed steel pipes for sour gas fields, *Proc. Int. Conf. on Pipeline Reliability, Calgary, June 2–5, 1992*, Houston, TX: Gulf, 1992, vol. 1, pp. 1–11.
11. Beloev, M., Khartung, F., Lolov, N., et al., Influence of structure and phase composition on the corrosion resistance of welded joints of duplex stainless steels, *Avtom. Svarka*, 2003, nos. 10–11, pp. 82–88.
12. Smirnov, M.A., Pyshmintsev, I.Yu., and Boryakova, A.N., Classification of low-carbon pipe steel microstructures, *Metallurgist*, 2010, vol. 54, nos. 7–8, pp. 444–454.
13. *Metals Handbook Desk Edition*, Davis, J.R., Ed., Materials Park, OH: ASM Int., 2006, 2 ed.
14. Chamov, S.V., Use of high-alloyed duplex steels in the petrochemical industry, *Khim. Tekhn.*, 2016, no. 2, pp. 37–39.
15. Shtremel', M.A., *Razrushenie. Kniga 2. Razrushenie struktur: monografiya (Destruction, Book 2: Destruction of Structures. Monograph)*, Moscow: Mosk. Inst. Stali Splavov, 2015.

Translated by Bernard Gilbert